




 Cite this: *RSC Adv.*, 2025, **15**, 22716

Terrestrial hermit crab with electronic payloads for opportunistic roaming environmental sensing†

 Brian Minsoo Lee,^a Holden King Ho Li,^b Ahjeong Son *^c and Beelee Chua *^a

We demonstrated the free roaming of a terrestrial hermit crab (*Coenobita* spp.) with a detachable harness accompanied by different payloads of sensors and electronics. The payloads tested are as follows: (i) an LED circuit with a switch, (ii) a solar-powered temperature and relative humidity sensor with wireless live data transmission, and (iii) a salt water sensing module for salt water detection. The acquired migratory data demonstrated that the hermit crab was able to map out the boundary between salt water and dry land in an arena, suggesting its applicability in monitoring coastal salt water ingress. Unlike conventional animal tagging, the harness conforms to the turbate pattern of shells *via* twisting motion, and the hermit crab can jettison the harness and payload at will by changing shells. This study explores the possibility of having hermit crabs as partners to pick up and randomly deploy sensors for opportunistic data acquisition without human intervention. They could function as a self-sustained roaming platform for detachable electronics.

 Received 19th May 2025
 Accepted 19th June 2025

DOI: 10.1039/d5ra03509k

rsc.li/rsc-advances

Introduction

Environmental sensing has become an indispensable and integral part of our collective endeavor to understand our natural and anthropologically influenced surroundings. At the rudimentary level, it provides insights into physical parameters such as temperature and relative humidity as well as chemical signatures such as pH and water salinity.^{1–3} With the advent of chemical and biological sensors, it is now possible to detect a myriad of chemical compounds and pathogenic microbes.^{4–9} Thus far, numerous efforts have been directed at improving sensor sensitivity and selectivity. However, sensors are only as informative as their mode of deployment. The common modes of deployment include static, vectored, and roaming, each with its own advantages and limitations. Static deployment situates a sensor in one fixed location. Spatial resolution can be improved using an array of static sensors.^{10,11} Vectored deployment requires moving sensors along a predetermined trajectory during sensing. This necessitates a mode of transport for the sensors, often in the form of an expensive remote control or autonomous vehicle (*i.e.* robot, drone, *etc.*).^{12,13} The alternative to vectored deployment is roaming deployment, where the vehicle is allowed to randomly walk instead.^{14,15} As compared to

static deployment, vectored and roaming deployment can monitor a large area without the need for a large number of sensors.

One of the key advantages of roaming deployment is that it prevents the need for a human pilot to guide it remotely or have an in-built autonomous navigation system. Unlike static sensors, it does not require an array to achieve higher spatial resolution. However, roaming deployment does require boundary markers, and therefore, the vehicle does not roam beyond the monitoring area. Unless it is self-replenishing (*i.e.* solar powered), it needs to be re-fueled or recharged periodically to keep roaming. In other words, robotic platforms may not be the most appropriate vehicles to deploy roaming sensors.

Given the above requirements, a persuasive line-of-inquiry would naturally lead us to the use of local wildlife as the vehicle for the roaming deployment of sensors. Notably, tagging wildlife with a global positioning system (GPS) to monitor their hunting range or migration paths has long been an established practice.^{16,17} For example, blue whales under study will have fin tags, while elusive wild cats wear collar tags. Animal-borne instrumentation could close observational gaps that have been previously in the blind spot of conventional equipment.¹⁸

Unfortunately, securing tags or sensors directly to the animal has its own ethical dilemma and demerits. For example, the animal can easily outgrow a collar or develop an infection at the tagged site. More importantly, the animal is often first trapped and sometimes sedated to facilitate sensor attachment. On occasions, recapturing might even be necessary. Nonetheless, there still exists a possibility of partnering with ecologically native wildlife for roaming sensing without the above-mentioned drawbacks. The terrestrial hermit crab is a unique land crustacean with a non-biologically attached shell.

^aSchool of Electrical Engineering, Korea University, 145 Anam-ro, Seongbuk-gu, Seoul 02841, Republic of Korea. E-mail: bchua@korea.ac.kr; chuabeelee@gmail.com
^bSchool of Mechanical and Aerospace Engineering, Nanyang Technological University, 50 Nanyang Avenue, Block N3, 639798, Singapore

^cDepartment of Environmental Science and Engineering, Ewha Womans University, 52 Ewhayeodae-gil, Seodaemun-gu, Seoul 03760, Republic of Korea. E-mail: ason@ewha.ac.kr; ahjeong.son@gmail.com

 † Electronic supplementary information (ESI) available. See DOI: <https://doi.org/10.1039/d5ra03509k>


In this study, we present a design strategy and demonstration that will allow us to partner with a native invertebrate animal for the roaming environmental sensing suitable for coastal ecology. The said native animal is the terrestrial hermit crab (family: Coenobitidae). The *Coenobita* genus has more than fifteen known species that are distributed across the tropical and sub-tropical coastlines of the world. Unlike their aquatic cousins, they spend a considerable period of their adulthood on coastal lands. In the absence of hardened exoskeleton to cover its soft abdomen, they have evolved to carry empty gastropod shells (*i.e.* that of marine snails) and hide within them for protection (Fig. 1a). As they grow larger, they will abandon the old smaller gastropod shells for larger ones. In other words, a terrestrial hermit crab will carry a shell at all times – a shell that is not biologically attached to its body. The shell is completely detachable (Fig. 1b). This presents a unique opportunity for us to enlist the terrestrial hermit crab to courier sensors and electronics without the usual ethical implications. In this work, we explore the design considerations and specifications for the endeavor. Specifically, it is important to consider

the terrestrial hermit crabs' less well-known behavior such as shell sculpting, as well as potential long-term implications.

The proposed design strategy involves housing a sensor and electronics on a minimally intrusive harness. The harness can be attached easily to shells of different sizes without inhibiting the hermit crab's motion. The robustness of the harness was characterized by pendulum-motion-driven tug force tests as well as ingress protection rating tests. Three types of payloads were also designed or sourced to demonstrate the feasibility of the strategy. The payloads are as follows: (i) an LED circuit board, (ii) a solar-powered wireless temperature and humidity sensor, and (iii) a salt water sensing module. In particular, the LED circuit board and salt water sensing module were custom-designed and fabricated, such that they are sufficiently miniaturized to fit on the harness. They are also sufficiently lightweight for the hermit crab to courier without motion inhibition. This study culminates with a roaming hermit crab deployed in an arena to demonstrate the mapping of salt water ingress by carrying the salt water sensor module as the payload.

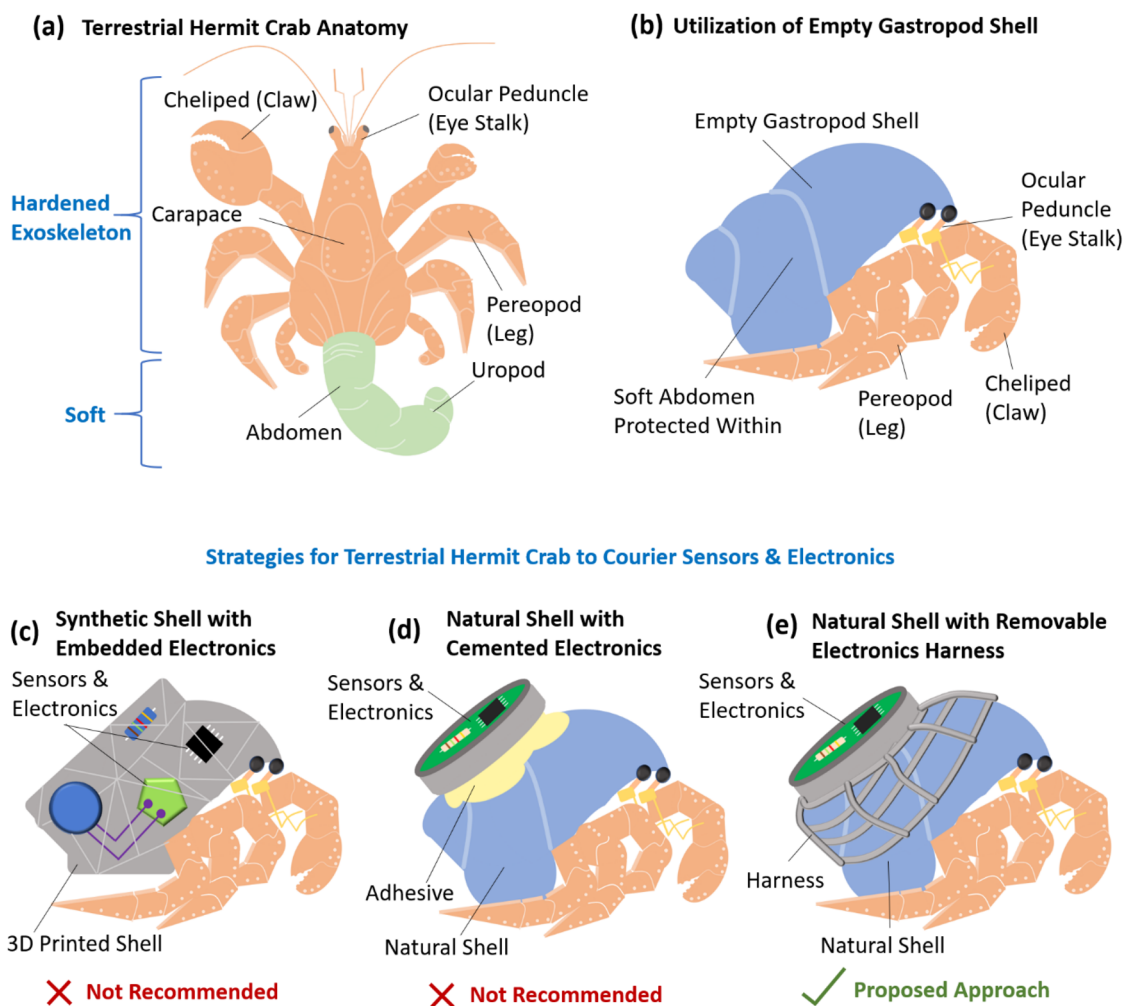


Fig. 1 (a) Anatomy of terrestrial hermit crab. It shows the hardened exoskeleton and soft abdomen. (b) Utilization of an empty gastropod shell where the soft abdomen is protected. Strategies for terrestrial hermit crab to courier sensors and electronics: (c) 3D-printed synthetic shell (not recommended), (d) attaching sensors and electronics via adhesives to natural shell (not recommended), and (e) attaching sensors and electronics via a detachable harness (recommended).



Design

Approaches, requirements, and selection

The prime consideration for this study is the sensor mounting and removal with minimal disruption to the hermit crab and its surrounding ecology. We first considered two evident design approaches for the sensors to be couriered by the hermit crab.

The first approach is conventional wisdom and involves the creation of a synthetic shell in its entirety (Fig. 1c). This synthetic shell may be designed with in-built sensors and/or enclosure for sensors. It is important to note that the creation of synthetic shells for hermit crabs is not new. Prior examples include glass-molded as well as 3D-printed shells. In the absence of natural shells, hermit crabs are known to take up residence in pseudo-shells such as small plastic containers.¹⁹ At first glance, the advantages of synthetic shells appear enticing. After all, it is an opportunity to utilize the entire shell structure and imbue it with sensing and other engineering functionalities. However, hermit crabs are also known to modify their shells. For example, a hermit crab would sculpt grooves at the shell opening to accommodate its eye stalks. In addition, the shell is required to be smooth on the interior (*i.e.* surface roughness of mother-of-pearl). This suggests a maximum surface roughness of the order of a few micrometers.²⁰ Since the interior of the natural shell consists mostly of fine aragonite and calcite (CaCO₃ polymorph) layers, the hermit crab also consumes it to supplement its calcium intake.²¹ However, the shell exterior needs to be coarsely textured as it helps the hermit crab to lodge itself among vegetation and rocks during rest. Furthermore, the natural shell is waterproof, so that it holds water within. This allows the hermit crabs' gills to stay moist and breathable.

Considering the above-mentioned requirements, the synthetic material used in this approach needs to be sufficiently pliable, comprising edible calcium compounds, possesses a smooth interior and coarse exterior, and stays water-proof. In fact, the natural shell is a remarkable but poorly understood feat of molluscan mineralization – the calcification and self-assembly of proteins, glycoproteins, and polysaccharide matrixes.²² Most importantly, this approach also mandates the eviction of the hermit crab from the synthetic shell during sensor removal. Given these considerations, it is unequivocally more ethical and convenient to simply base the design on natural shells instead of creating synthetic ones.

This leads us to the second approach that involves the fixation of sensor and electronics enclosure onto the natural shell. Permanent fixation of the enclosure onto the natural shell has the same sensor removal issue as mentioned earlier (Fig. 1d). Hence, the enclosure should be fixated on the natural shell *via* a detachable harness (Fig. 1e). The design of the harness has several key requirements. An evident requirement is the ease of attachment and detachment without shell encircling features (*i.e.* girth). Such a feature may snare on debris and entrap the hermit crab. In addition, the harness should not interfere with motion, and therefore, the mimicking of natural forms is preferred. Furthermore, the harness should not shift position while remaining attached to the natural shell. A dislocated

harness should detach and not result in an unnatural shell form, which interferes with motion. Finally, the hermit crab should have a chance of jettisoning the harness at any time. Table 2 summarizes the design requirements for the harness.

Mathematical ratio spirals and universal fit harness

Fig. 2a–c show a natural shell that belongs to a marine snail (*Turbo* spp.). It is one of the natural shell types favored by the terrestrial hermit crabs. It is compact and has a ball-like profile, which minimizes the cross-section profile of the hermit crab. In this way, it can pass through small openings in the ground or vegetation. It also enables a quick getaway from aerial predators by dropping from the elevation and rolling away into the underbrush. The size of the shell is often characterized by the operculum length (Fig. 2b).

The turbinat pattern of the shell has a particular significance. Each subsequent quarter spirals away from the center with an increasing radius, probably in accordance with a mathematical sequence analogous to that of the golden ratio or meta golden ratio as reported by Bartlett 2018 (Fig. 2d and e).²³ In this case, the ratio is ~ 1.114 as compared to 1.618 of golden ratio and 1.356 of meta golden ratio (Fig. 2f). As the turbo snail grows, its shell gets extended and becomes larger at the opening. This leaves the already formed segments in its original dimensions. In other words, the shell geometry from the tip of the shell will always be the same regardless of the turbo snail's age.²⁴ This allows us to design a harness with the universal fit regardless of the turbo shell size. The harness design consists of form hugging and pliable mesh that conforms to the smallest five spirals of the turbo shell. This allows the harness to be twisted on and off the turbo shell (Fig. 2g). An enclosure is also formed over the harness, so that sensors and electronics may be accommodated.

Materials and methods

Prototyping harness and enclosure

Harness prototype I was constructed by thermoforming a high-density polyethylene (HDPE) mesh (mesh thickness = 2 mm, mesh opening = 10 mm × 3 mm mesh) over a vacant turbo shell (Fig. 2h–m). The heat was supplied by a heat gun (GDT-1001A, Goldtool Co. Ltd, Taiwan). After the harness was formed, it was allowed to cool *in situ* on the shell. Once the harness has cooled and hardened, it was removed from the shell. The edges of the harness were selectively trimmed to ensure a secure fit and ease of installation. A round acrylic enclosure with a screw-on lid (height = 12 mm, diameter = 35 mm) was used as the sensor and electronics enclosure and attached *via* a glue gun (FOG280, Mono Glue Gun, Korea) (Fig. 2n and o). The overall weight of the harness and attached enclosure was ~ 13 g. Notably, the enclosure was mounted such that the sensors and electronics were away from the operculum to minimize interference to the hermit crab's motion. This prototype formed the basis for 3D scan.

Harness prototype II was based on the 3D scan of the harness prototype I (Fig. 3a). The sensor enclosure was designed using



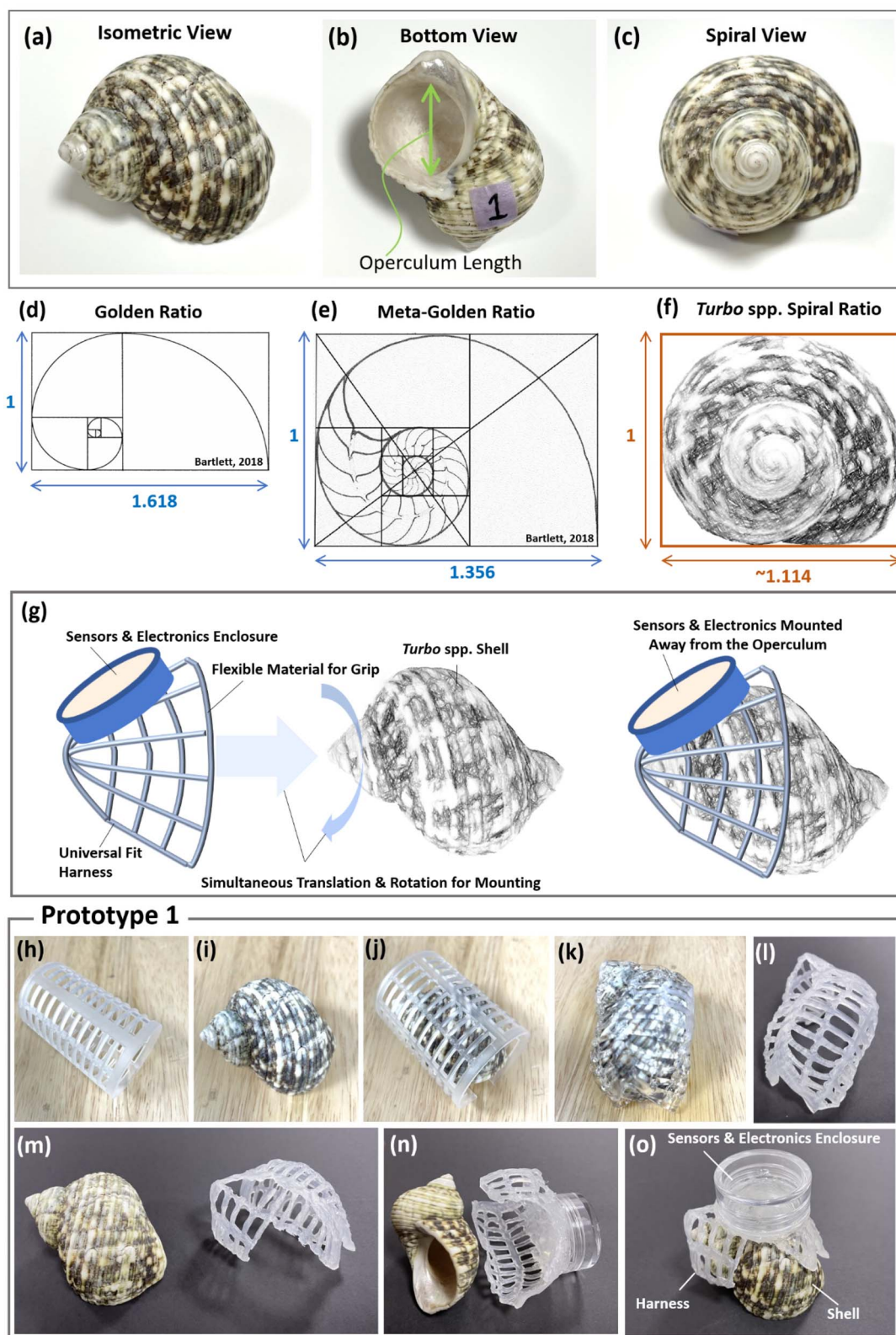


Fig. 2 (a–c) Photographs of natural turbo shells. (d) Golden ratio. (e) Meta-golden ratio. (f) *Turbo* spp. Spiral ratio. (g) Detachable harness conceptual design. (h–o) Step-by-step thermofforming of harness prototype 1 with the sensor and electronic enclosure.

SolidWorks (student version 2022) and integrated with the scanned harness using Blender (version 3.5) (Fig. 3b). Particular care is taken to smooth out the interface between the harness

and the sensor enclosure to limit the radius of curvature to no less than 2 mm (Fig. 3c–e). The harness prototype II is subsequently 3D printed (conventional fused filament fabrication)



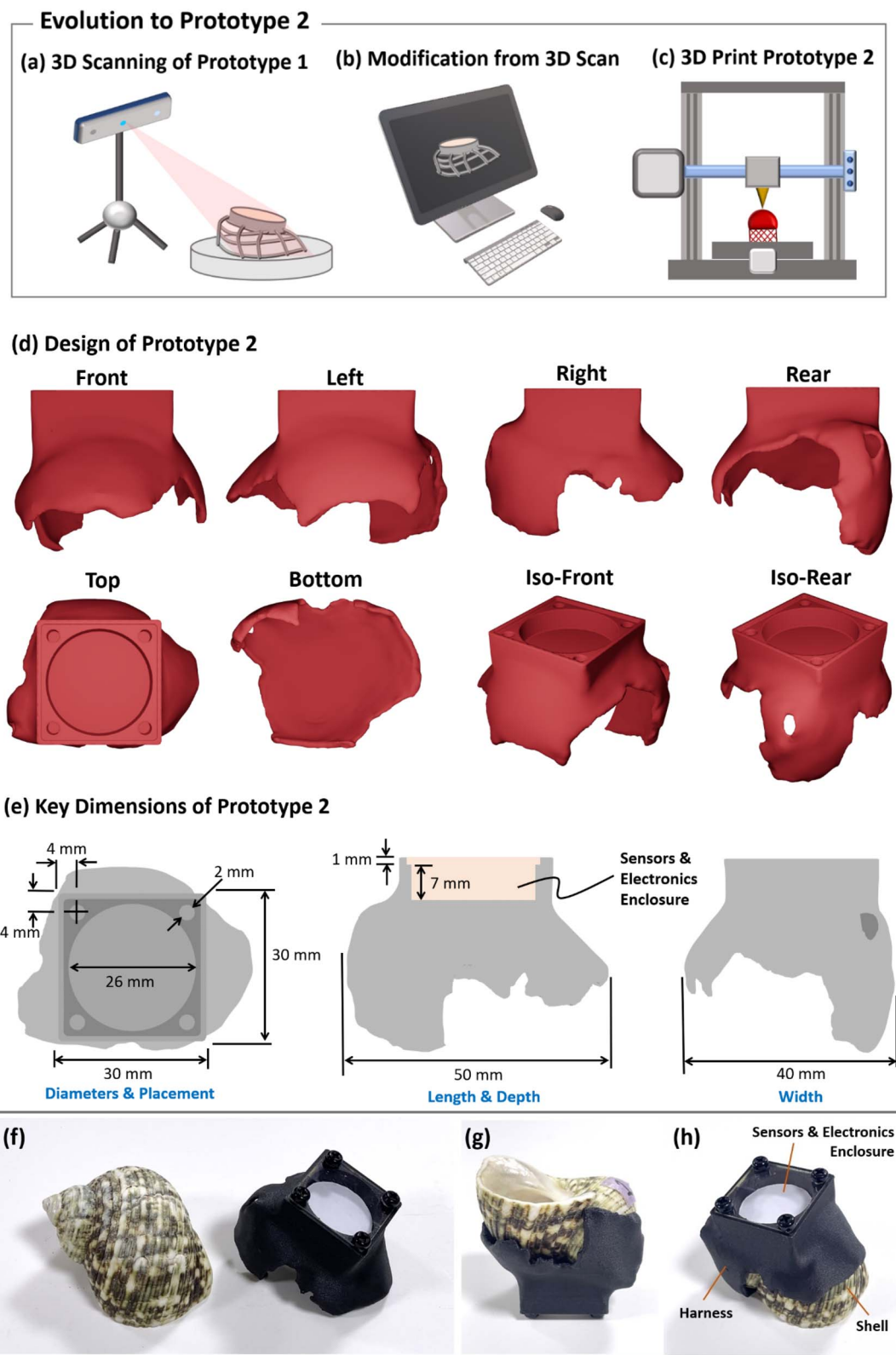


Fig. 3 (a–c) Evolution from harness prototype 1 to 2. (d) Design of harness prototype 2. (e) Key dimensions of harness prototype 2. (f–h) Photographs of harness prototype 2 with the natural shell.

using an Onyx® carbon–nylon composite filament (Markforged Inc, USA) on a 3D printer (Cubicon 3DP-310F, AMR Europe B.V., The Netherlands). It is noteworthy that the mechanical

properties of the said composite have been extensively characterized by Lee *et al.* 2023.²⁵ It can withstand over 1200 N of tensile force for a single printed layer. It is also highly resistant



to abrasion. Corrosion resistance to seawater is also exemplified by its use for 3D-printed components on unmanned surface vehicles. The sensor enclosure lid was cut from a 1 mm acrylic sheet using a laser cutter (Model PLS 150D, Universal Laser Systems Inc, USA). It was secured to the sensor enclosure using M3 Philip head screws (Fig. 3f). An initial fit was performed on a single shell, as shown in Fig. 3g and h. The harness prototype II was the final design iteration in this study and used for subsequent experiments. The STL file for harness prototype II may be provided upon request. Alternative material candidates for the harness can be cellulose-based composites that allow freeform shapes with high fracture toughness. It should be noted that while a mesh-like design could reduce the overall weight of the harness, it could also generate localized stresses, which might induce layer delamination in a 3D-printed part.

Fit and tug test on different shell samples

Six shell samples (Fig. S1†) were measured and weighed (Digital Scale Model CPS-01, CPLB Co. Ltd, China). The size and weight of the shells are shown in Table 1. The weight of the shells ranged from 36 to 47 g. The fit and tug test was performed by attaching the harness and shell to the end of a pendulum (Fig. 4a–c). By releasing the pendulum from an initial position given by a launch angle θ , the shell would experience a centrifugal force (in addition to gravitation force) that pulls it away from the harness (Fig. 4d). The centrifugal force F (also the tug force) was calculated as follows:

$$F = m\omega^2 L \quad (1)$$

where m is the mass of the shell, ω is the radial velocity, and L is the pendulum length (~ 300 mm). The radial velocity ω was calculated from the tangential velocity V_t . As shown in Fig. 4e, it is, in turn, calculated from the energy conservation between maximum potential and kinetic energy as follows:

$$\omega = \frac{V_t}{L} \quad (2a)$$

$$V_t = \sqrt{2gh} \quad (2b)$$

$$h = L(1 - \cos \theta) \quad (2c)$$

where g is the gravitational acceleration of 9.81 m s^{-2} . The launch angles θ employed for the tests were 36.7° and 90° . Each of the shell samples was tested 5 times. It should be noted that the higher launch angle would induce a higher centrifugal force

Table 1 Characteristics of shell samples

Shell	Weight (g)	Operculum length and width (mm)	Length (mm)
1	47	27.0 × 25.5	49.5
2	46	22.2 × 25.1	47.5
3	38	22.3 × 23.5	45.1
4	46	26.8 × 25.9	47.6
5	36	22.8 × 21.9	45.0
6	36	23.3 × 23.0	44.8

F for the same shell and harness pair. Any shell and harness pair that disengaged at a launch angle of 36.7° would not be subjected to further testing at 90° . The ability to withstand the tug force at 90° launch angle would indicate the harness's ability to hold the combined weight of the shell and the hermit crab.

Ingress protection tests and ratings

Table S1† shows the ingress protection ratings commonly employed by electronic device manufacturers. It describes the different protection levels against water (such as droplet, spray, and submersion) as well as solid bodies (such as fingers, sand, and dust). The harness was evaluated for its ingress protection. It was first placed in an acrylic test box prior to exposure to soil mixture or water spray (Fig. 5a–c). As shown in Fig. 5d, the soil mixture (Daedong Industrial Co. Ltd, Korea) is a matrix of mostly coco peat ($\sim 67\%$) and its composition is shown in Table S2.† During the test, the soil mixture (~ 8 g) was scattered over the harness and then removed for examination (Fig. 5e and f). For the water ingress test, a dry paper disc was placed within the sensors and electronics enclosure in the harness. A wet paper disc after test would suggest an ingress event (Fig. 5h and i). During the test, the harness was sprayed with ~ 2 mL of water and excess water was wiped off the protective cover prior to visual inspection. Photographs were taken before and after the tests for comparison. A total of three harnesses were tested.

Payload designs and tests

As shown in Fig. 6a, payload #1 is a simple LED circuit powered by a lithium battery (CR1220, 3 V, Panasonic Energy Co. Ltd, Japan). It is buffered by a $1 \text{ k}\Omega$ series resistor and controlled by a sliding switch. Its purpose is to suggest the possibility of a live electronic circuit payload on the hermit crab and to identify immediate catastrophic failure modes such as electromagnetic disturbance on the hermit crab as well as circuitry malfunction from movement-induced knocks.^{26,27}

Payload #2 is a commercially available solar powered temperature and relative humidity (RH) sensor (CYALKIT-E02 Solar-Powered BLE Sensor Beacon, Cypress Semiconductor Inc, CA, USA). It uses a monolithic temperature and relative humidity sensor chip (Si7020-A20-GM1, Silicon Labs), and has a temperature accuracy of $\pm 0.4^\circ \text{C}$ and a relative humidity accuracy of $\pm 4\%$. As shown in Fig. 6b, it fits within the sensor and electronics enclosure of the harness. The clear acrylic allows payload #2 to be powered *via* ambient light, while transmitting environmental data wireless *via* the Bluetooth low-energy (BLE) protocol. During the experiment, payload #2 was couriered by the hermit crab, while the data were relayed to the nearby BLE transceiver (connected to a computer). Simultaneously, the ambient temperature and relative humidity were manually recorded using a standalone digital thermometer/hygrometer (KTJ TA218B, China).

Finally, payload #3 is a salt water sensing module that consists of two sensing probes, a bipolar junction transistor (2N5551, Fairchild Semiconductor Inc, USA), three resistors ($R_1 = 680 \Omega$, $R_2 = 270 \Omega$, $R_3 = 1 \text{ k}\Omega$), a lithium battery (CR2032, 3 V, Toshiba Corp., Japan), and a blue LED salinity indicator (Fig. 6c). In brief, an open circuit (absence of salt water) between



Fit & Tug Test

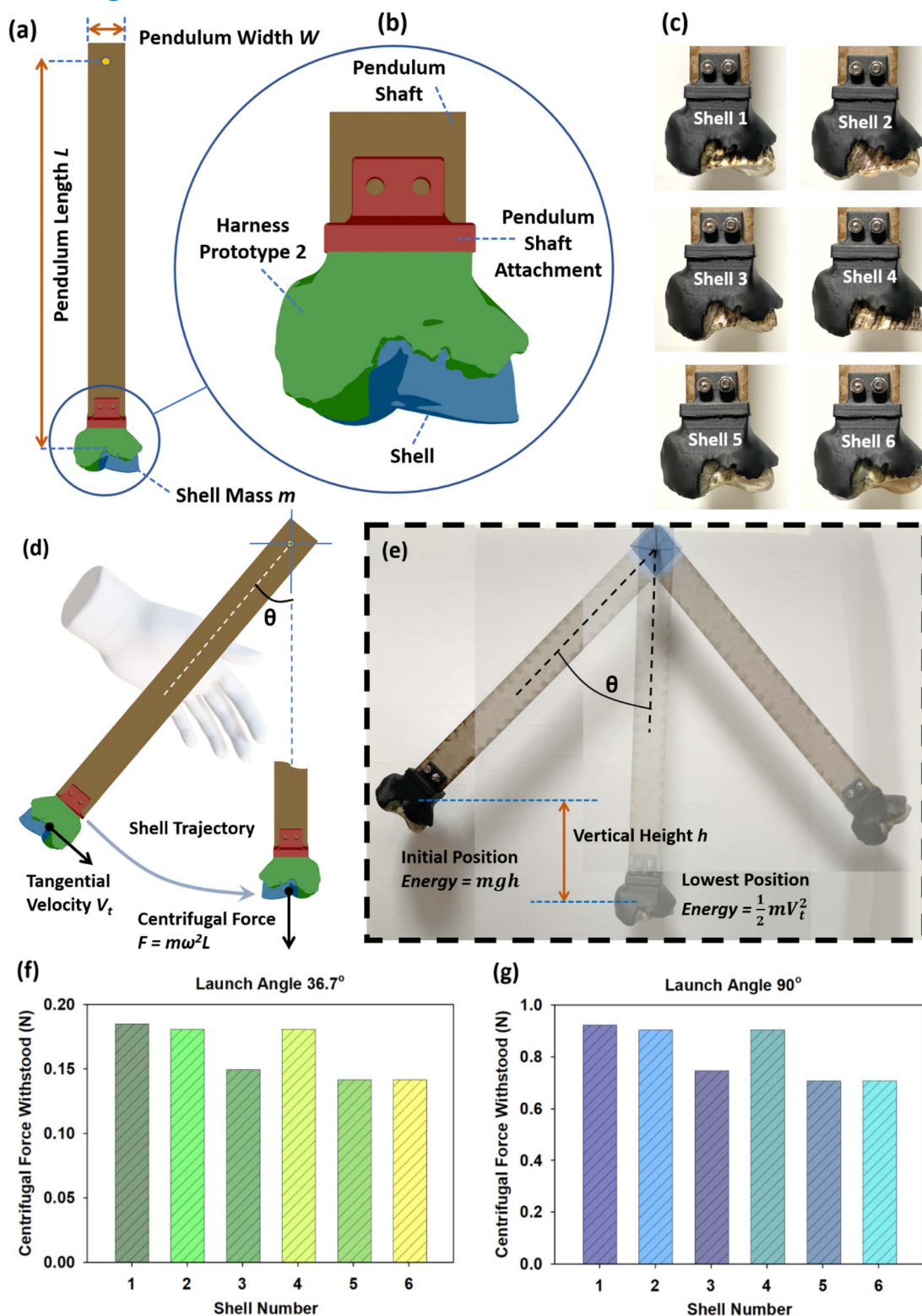


Fig. 4 Fit and tug test: (a and b) pendulum test setup design. (c) Photographs of harness prototype 2 fitted over six different shell samples. (d and e) Underlying mechanics of tug test. (f and g) Results from tug test using different shell samples and launch angles.

the sensing probes results in a low base-emitter voltage of the transistor. This means the transistor is in an “off” state and does not permit the electrical current to pass through the LED

(unlit). In the presence of salt water between the sensing probes, the transistor’s base-emitter voltage becomes high and the transistor transits into an “on” state. It allows electrical current



Ingress Protection Test

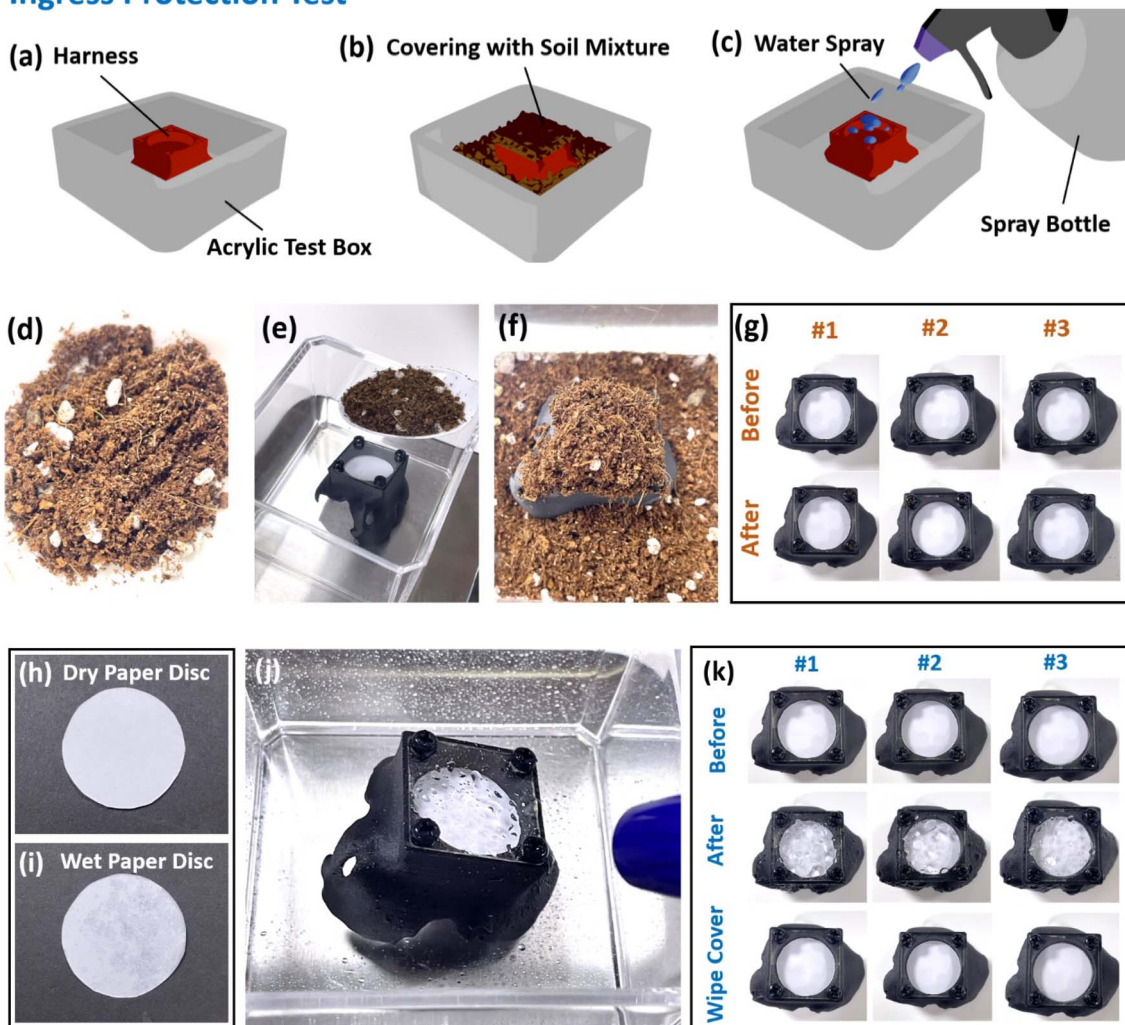


Fig. 5 Ingress protection test: (a–c) steps depicting soil mixture and water spray exposure. (d) Soil used in ingress test. (e) Soil ingress test setup. (f) Harness prototype 2 covered in soil mixture. (g) Soil ingress results of three harnesses showing no observable ingress. (h) Dry paper disc prior to water exposure. (i) Wet paper disc after water exposure. (j) Harness prototype 2 sprayed with water. (k) Water ingress results of three harnesses showing no observable ingress as the paper discs remained dry.

to pass through the LED and, thus, causes it to light up. To characterize the electrical conductivity/salinity required to light up the LED, it is exposed to a water sample with different electrical conductivities (blank, 0.01, 0.05, 0.075, 0.1, 0.4, 0.8, and 1.0 M phosphate buffered saline or PBS). The corresponding electrical conductivities are shown in Table S3† as established in a previous study.²⁸ It should be noted that the design of the salt water sensing module does enable differentiation of different salt water conductivities. This is because so long as the transistor operates in the active region, the resulting electrical current will correspond to the salt water conductivity.

Terrestrial hermit crab

Coenobita brevimanus, commonly referred to as Indos, was employed as the terrestrial hermit crab to carry the different payloads. The hermit crab is approximately 10 years old and weighs ~67 g with the shell. This shell is slightly larger than the

six shell samples and, hence, heavier. It was rescued from local pet trade and kept by one of the corresponding authors since 2019. Its natural habitat spans from the East African coast to the South Pacific, and it is found as far north as the Japanese archipelago. Since it breathes *via* moist gills, it is critical that the experiments are conducted with an ambient relative humidity of at least 60%. Therefore, the experiments were conducted during the month of July 2024 in Korea Peninsular, where the temperature and relative humidity approximate to that of tropical conditions. During the experiments, the ambient light was kept dim to minimize moving shadows and hence stress to the hermit crab.

Salt water ingress mapping using roaming hermit crab with payload #3

The electrical conductivity calibration curve for salt water was first constructed by measuring the electrical conductivity using



Payload Test

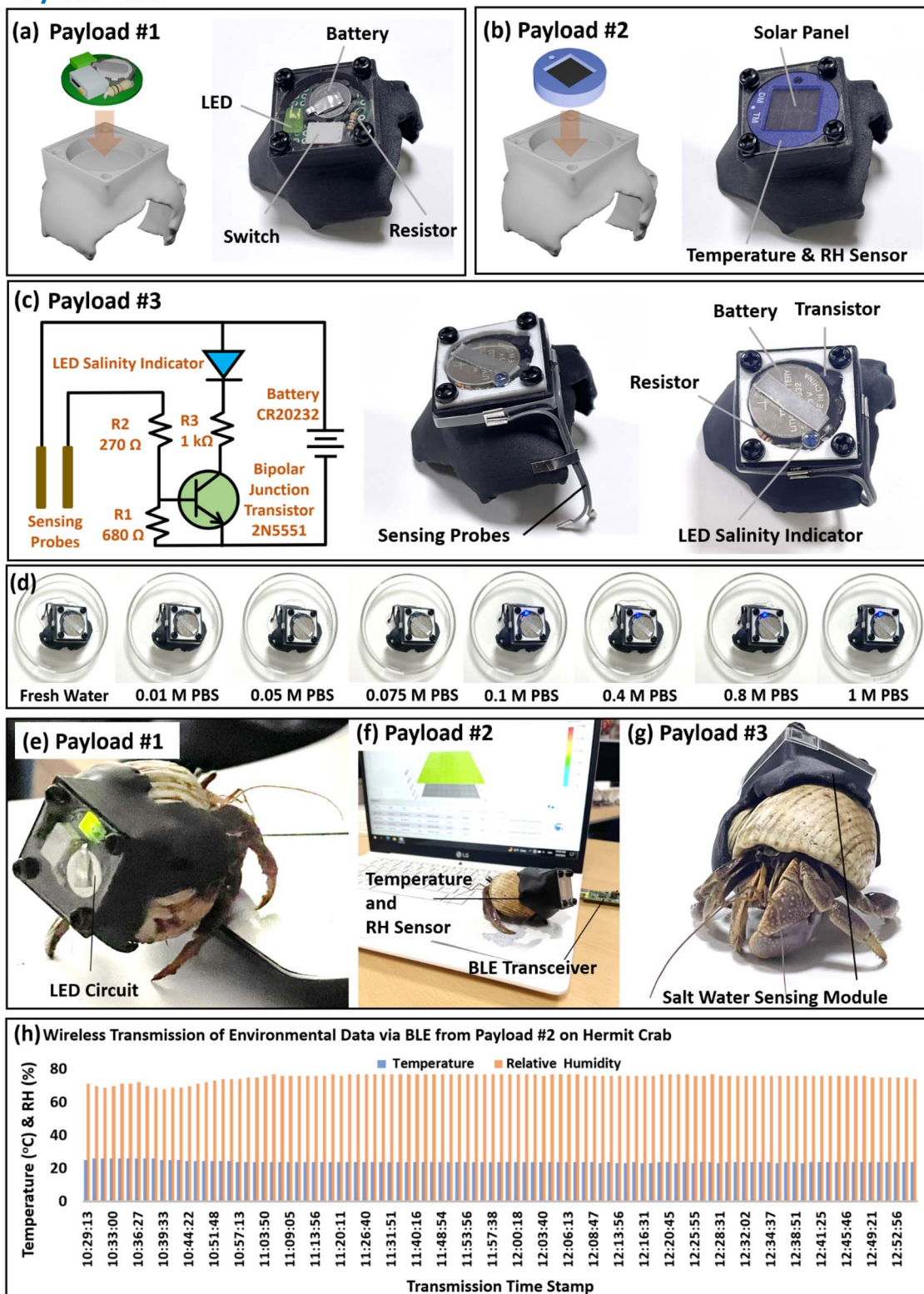


Fig. 6 Payload test: (a) payload #1 is a battery-powered LED circuit. (b) Payload #2 is a solar-powered temperature and relative humidity sensor. (c) Payload #3 is a salt water sensing module. (d) Response of payload #3 to the fresh water and phosphate saline buffer of varying molarity. It shows that payload #3 is able to detect the transition from 0.075 (~1125 $\mu\text{S cm}^{-1}$) to 0.1 M PBS (~1845 $\mu\text{S cm}^{-1}$). This also corresponds to the transition from fresh water to salt water. (e) Hermit crab courier payload #1, with the LED on. (f) Hermit crab courier payload #2, with the sensor wirelessly transmitting live temperature and relative humidity data. (g) Hermit crab courier payload #3, with the sensing probes contacting the ground. (h) Environmental (temperature and relative humidity) data wirelessly transmitted by the hermit crab payload #2 for 2.5 h.



a conductivity meter (EC-98306, Yieryi Technology Co. Ltd., China) with incremental addition of sea salt (Fig. 7a). This informs that salt water (simulating sea water) with an electrical conductivity of $\sim 3000 \mu\text{S cm}^{-1}$ could be formulated by adding 1725 mg of sea salt to 1 L of filtered water. It should be noted that fresh water typically has electrical conductivities ranging from 0 to $1500 \mu\text{S cm}^{-1}$.

A custom arena ($0.45 \text{ m} \times 0.45 \text{ m} \times 0.40 \text{ m}$) was constructed with 5 mm-thick Plexiglass (Fig. 7b). It was approximately divided by half using a 20 mm tall barrier to construct a half-moon-shaped salt water pool as well as dry land. One liter of the previously formulated salt water was used to fill one half of the arena, while the other half was covered in a shredded coconut husk (Fig. 7c).

In every salt water ingress mapping experiment, the hermit crab (with payload #3) was first placed in a salt water pool of the arena. A video recorder was positioned above the arena and the ambient lighting was dimmed. The hermit crab was allowed to roam in the arena for ~ 15 to 20 min. During this time, the hermit crab would roam freely between the salt water pool and the dry land. The LED salinity indicator would turn on whenever the hermit crab was in salt water pool. The experiment was performed five times.

Results and discussion

Fit and tug test on different shell samples

As shown in Fig. 4c, the harness was able to fit all six different shell samples regardless of their sizes. It was able to grip and hold the weight of all the shell samples (36 to 47 g). For the launch angle of 36.7° , the applied tug forces ranged from ~ 14 to 18 g (Fig. 4f and Table S4[†]). There was no dislodgement observed for all the harness and shell pairs, and hence, they were further subjected to the higher tug force at 90° . As shown in Fig. 4g and Table S1,† all the harness and shell pairs were able to withstand tug forces ranging from ~ 71 to 92 g. This means the harness could withstand the conservatively high combined weight of the shell and hermit crab.

This indicates that the harness can be secured to hermit crab shell *via* mechanical/frictional gripping without the risk of slippage and disengagement from motion. At the same time, it can still be removed safely from the shell without causing any damage to the shell or the hermit crab. More importantly, in the event that the harness is lodged between rock crevices or vegetation debris, the hermit crab is also expected to be able to free itself by rotating the shell out of the harness. It should be noted that the grip of the harness on the shell was not tested to failure because it was not a necessary metric for the demonstration.

Ingress protection rating

The visual inspection of the harnesses before and after the soil mixture ingress test is shown in Fig. 5g. There was no visible ingress of soil mixture into all three harnesses. There was some residual soil on the exterior of the harnesses, especially along the acrylic protection cover gap and on the screws. Similar

observations were made with water ingress tests. As shown in Fig. 5k, the visual inspection of the paper disc within the sensor and electronics enclosure did not indicate water penetration. Based on the ingress protection ratings, IEC 60529 (corresponds to European Standard EN60529) shown in Table S1,† the harness's sensor and electronics enclosure is able to prevent ingress of soil mixture and water spray, and therefore, demonstrates an ingress protection rating equivalency of IP53.

Payload tests

The functional check for payload #1 was relatively easy to perform, and is shown in Fig. 6e. The presence of the harness and payload #1 did not impede the hermit crab's movement at all. Payload #1 was powered (green LED on) during the hermit crab's random walk. It was able to haul payload #1 around without compromising on its circuit's functionality (green LED remained on). The knocks induced by the hermit crab's movement did not have an immediate effect on the circuit interconnects. There was also no immediate rejection of the harness and payload by the hermit crab due to possible electromagnetic disturbance.

The hermit crab's response to payload #2 was very similar to that with payload #1. It did not impede its movement and was able to roam freely. With payload #2 onboard, the hermit crab roamed freely for ~ 2.5 h while transmitting temperature and relative humidity (RH) data wirelessly back to the computer *via* its Bluetooth low energy (BLE) transceiver (Fig. 6f). The wireless transmission of environmental data was uninterrupted for the duration of the test. The data showed a temperature range of 23.2 to 25.9°C and a relative humidity range of 68 to 77% (Fig. 6h and Table S5[†]). It agrees with the standalone thermometer/hygrometer readings of 25.7 to 26.0°C and 61 to 63%. It should be noted that the natural habitat of the terrestrial hermit crabs lies in the subtropical and tropical parts of the world. The temperature ranges from approximately 15°C (winter in the subtropics) to 32°C (in the equatorial or summer in the subtropics). The relative humidity will be at least 70%. While the sensor itself can be subjected to rapidly changing temperatures and relative humidity, it is not advisable to subject the hermit crab to the same rapidly changing temperatures. Therefore, an experiment to include the full seasonal temperature swing need to be conducted over the natural season cycle and outdoors, necessitating a separate larger study.

The characterization of payload #3 (salt water sensing module) with fresh water as well as phosphate buffered saline (of different molarities, Table S3[†]) is shown in Fig. 6d. As expected, the LED salinity indicator did not turn on upon contact with fresh water (electrical conductivity = $131.4 \pm 2.1 \mu\text{S cm}^{-1}$). It remained off with increasing molarity from 0.01 to 0.075 M PBS (electrical conductivity = $1125.3 \pm 1.5 \mu\text{S cm}^{-1}$). The LED salinity indicator finally lit up with 0.1 M PBS (electrical conductivity = $1845.7 \pm 1.2 \mu\text{S cm}^{-1}$). This means that payload #3 is able to distinguish the transition of electrical conductivity from ~ 1125 to $1846 \mu\text{S cm}^{-1}$. Recall that the electrical conductivity of fresh water ranges from 0 to $1500 \mu\text{S cm}^{-1}$, implying that payload #3 will be able to detect a surface



Salt Water Ingress Mapping

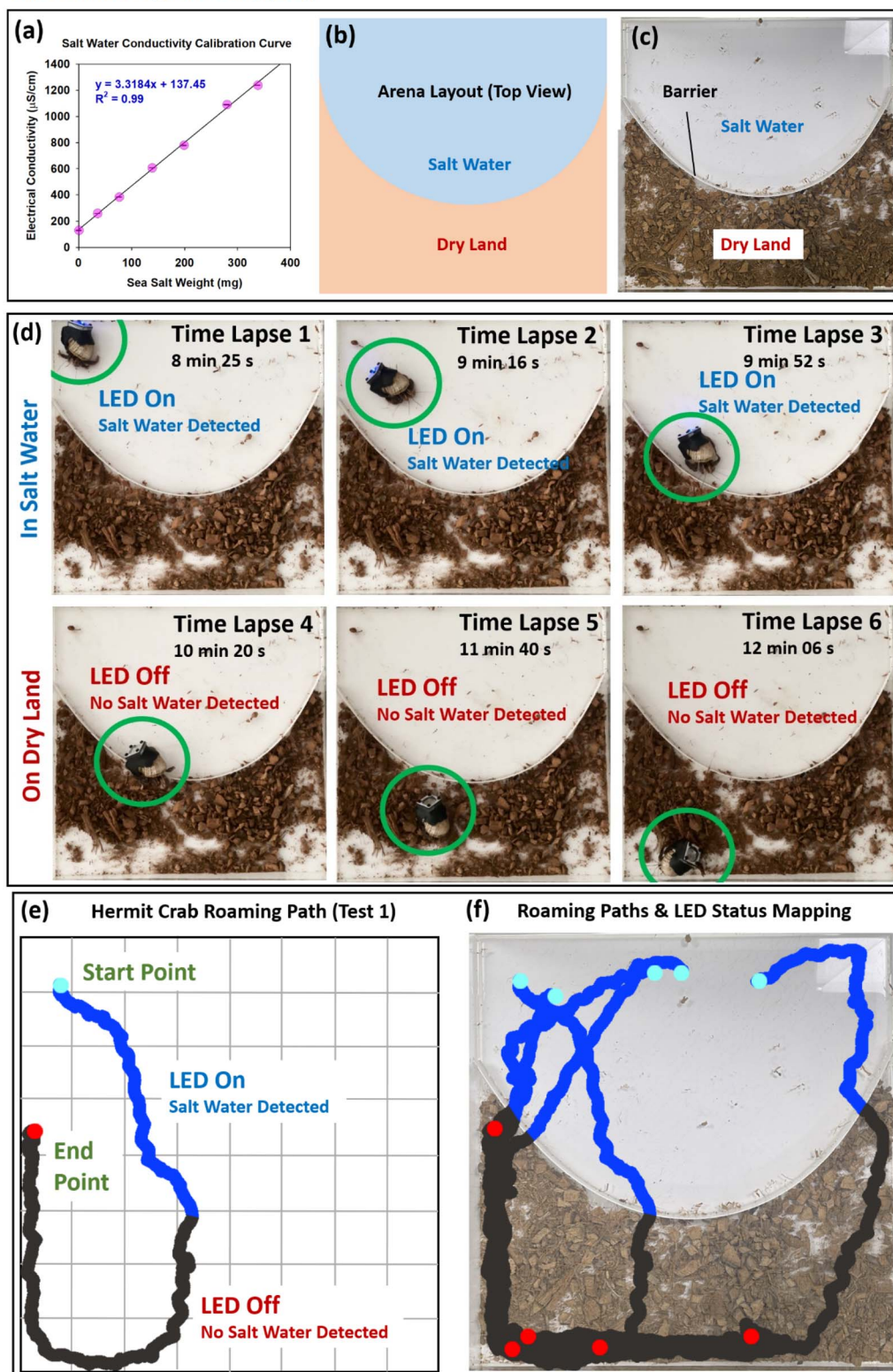


Fig. 7 Salt water ingress mapping: (a) salt water conductivity calibration curve used for formulating salt water ($\sim 3000 \mu\text{S cm}^{-1}$) in the arena. (b and c) Arena layout with salt water and dry land separated by a barrier. (d) Time-lapsed video images of hermit crab with payload #3 roaming in the arena (test 1). The LED salinity indicator was lit while the hermit crab was in the salt water. As it transverse over to dry land, the LED salinity indicator is switched off. (e) Roaming path of the hermit crab with payload #3 (test 1) and the corresponding LED status. (f) With repeated roaming runs over the arena, the hermit crab with payload #3 was able to map the salt water and dry land within the arena.



Table 2 Harness prototypes 1 and 2 and payload weights

Item	Weight (g)
Harness prototype 1	13
Harness prototype 2	10
Payload #1: LED circuit board	2
Payload #2: CYALKIT-E02 temperature & humidity sensor module	4
Payload #3: salt water sensor module (including CR 2032 battery)	6

environment that is definitely not of fresh water or dry land. As expected and similar to the previous two payloads, the hermit crab's movement was also not inhibited by payload #3 (Fig. 6g).

Salt water ingress mapping

The conductivity of salt water in the arena was 1238.0 ± 1.9 $\mu\text{S cm}^{-1}$ (Table S6†). Upon being placed in the arena, the hermit crab would take a few minutes to emerge from its retracted position and begin free roaming. As shown in the time lapse video capture from test 1 (Fig. 7d), the hermit crab would traverse across the arena from the salt water to dry land. The time duration between time lapse 1 and time lapse 6 was approximately 4 min. As it was walking over the salt water, payload #3 would detect the salt water and its LED salinity indicator would light up accordingly. As the hermit crab climbed over the barrier onto dry land, payload #3 no longer detected salt water and, thus, turned off its LED salinity indicator. Tests 2 to 5 also demonstrated the same consistent correspondence between the hermit crab's location in the arena and the status of the LED salinity indicator. The roaming path of the hermit crab as well as the LED salinity indicator status in each test is shown in Fig. 7e and S2.† The arena layout was further superposed over the roaming paths and LED salinity indicator status of all five tests (Fig. 7f). The boundary between salt water and dry land could be marked by the locations where the LED salinity indicator switched its status. In other words, the salt water boundary could be mapped by the roaming hermit crab with a salt water sensing module as payload.

It is important to note that salt water ingress along tropical coast lines cannot be mapped out by aerial drones due to the subterranean nature of the pathways as well as thick coastal tree canopy. The surface coastline may remain the same but the salt water ingress *via* subterranean pathways can change the salinity of inland fresh water bodies. Since terrestrial hermit crabs like *Coenobita brevimanus* are known to travel as much as 300 m inland from the coast lines, they will also seek out both fresh and salt water pools to balance the salinity in their gills. This makes them excellent candidates to sample water bodies around the coast lines. The harness and payload #3 can also provide additional behavioral insights into the hermit crab's routine of seeking out fresh and salt water pools.

Significance and limitations

Currently, roaming environmental sensing either mandates the use of mechanized vehicles such as drones and robots or the invasive/restrictive attachment of sensors to wildlife. The

mechanized approach is complex, cost-prohibitive, and therefore has limited accessibility to environmental scientists. However, the attachment of sensors to wildlife is potentially detrimental to their well-being due to damage and infection risk at the attachment sites. Sometimes, it also inhibits their movement and behavior. More importantly, it always requires the trapping, capture, and sometimes even sedation, to facilitate sensor attachment.

This study has demonstrated a new paradigm of roaming environmental sensing along coast lines that does not invoke the drawbacks of the previously mentioned approaches. The use of terrestrial hermit crabs has a myriad of advantages. First, payloads can be attached (*via* harness) to empty shells prior to planting them around the study area. This will allow hermit crabs to pick them up during shell swap. In that way, there is no need to perform capture and release of the hermit crabs. This eliminates the need for trapping. This also allows the hermit crab to decide if it wants to wear a shell with harness and payload. Second, the hermit crab can jettison the harness and payload at will simply by swapping the shell. This eliminates the need for human intervention in the event that the harness and payload obstruct the hermit crab's movement. This also means that should the harnessed payload become intolerable (due to excess weight, bulk, or even electromagnetic disturbance), the hermit crab will eventually abandon the harnessed payload together with the shell. In this case, abandonment of the harnessed payload does not constitute failure because it just stopped roaming temporarily. Most importantly, the hermit crab is not harmed. The harnessed payload always has the possibility to be picked up by a different hermit crab.

With the universal fit harness design, scientists can also work with a wide range of shell sizes with ease. The current version of the harness prototype might have appeared large as compared to the hermit crab shell. Fortunately, it is rather lightweight (approximately half of shell's weight). Furthermore, hermit crabs are known to prefer oversized shells and hence have evolved to carry much larger and heavier shells. Most importantly, hermit crabs can easily switch out the shells if they inhibit their movement.

The sensor and electronics enclosure can also be modified, if necessary, to accommodate a wide range of sensors and even geo-positioners. It is not limited to the three types of payloads, as demonstrated in this study. In addition, the temperature, relative humidity, and salt water sensor demonstrated in this study can be further integrated into a single package by packing the circuitry into application-specific integrated circuits (ASICs). With the advent of flexible electronics, it is not inconceivable to



have in-built circuitry and sensors even within the harness curved surface itself.^{29,30} For example, an array of screen-printed electrochemical or immobilized fluorescence sensors can be laminated over the harness surface to monitor environmental chemicals such as phthalates.^{4,9,31,32} In other words, by partnering with sensor-enabled hermit crabs, spatial sensing efficiency can be achieved as large study area can be monitored with a small number of roaming sensors. Given the appropriate sensors, the hermit crabs can also be partnered to monitor other parameters such as water turbidity, heavy metal and humic acid concentrations, bacterial and algal loads, as well as the presence of nitrogen compounds (indicative of fertilizer runoffs). It may be able to provide insights and early warning to foreboding environmental disasters. For example, a simultaneous increase in algal loads as well as nitrogen compounds may suggest an impending harmful algal bloom.

The key innovation of this work lies in partnering with hermit crabs for environmental sensing *via* a custom-designed removable harness as well as sensors. It is a feasibility study to lay foundation for a new sensing strategy where a small number of hermit crab-mounted sensors are able to cover a large study area *via* roaming. Both harness and sensors can benefit from future iterations and refinements. In particular, the sensor integration can benefit from the existing multi-sensor architecture.^{33–35} Hermit crabs are very cost-effective partners because they are native to the environment and exist in large numbers.

One of the evident potential limitations pertains to the recovery of the harness and payload. In the short term, the use of geo-positioners (such as those based on GPS) will facilitate the location of the harness and payload. The recovery itself will still require manual intervention or even occasional use of remote-controlled vehicles. It is also possible to outfit the harness with a floater, so that it will eventually be washed up to shore for recovery. Another potential issue relates to the material aspect of the harness. Ideally it should be ecologically friendly and perhaps fabricated using natural materials such as rubber, ceramics, and cellulose matrix. This could be realistically implemented with existing technologies.^{36,37} In the long run, it will be ideal to employ biodegradable or even edible electronics and sensors as payload. Despite its nascent development phase, researchers have already demonstrated the possibility of edible medical sensors, transistors, and even batteries.^{28,38–41}

The scale of the current demonstration is also relatively small (45 cm × 45 cm × 40 cm arena). Nonetheless, terrestrial hermit crabs in the wild are also known to traverse many miles in a single night. Therefore, it is reasonable to suggest that the terrestrial hermit crab remains amenable to large distance deployment. As for the terrestrial hermit crab's receptiveness to a shell with a foreign object (*i.e.* harness and sensor) attached, the terrestrial hermit crab is also known to use an assortment of containers as a shell surrogate (such as a plastic container, tin can or even a plastic doll's head, Fig. S3†).

It should be noted that in this work, re-iteration of long-range data acquisition of the payloads is not necessary because there already exist commercially available solutions

and protocols. An example is the ZigBee® protocol where data can be transmitted over a range of 10 km using a coin battery. The ZigBee® wireless transmitter Xb24-Z7sit-001 will fit on the harness. Another approach will be to use the ZigBee® long-range transmitter and receiver module nRF52840 MS88SF2.

Conclusions

This study has solved the long-standing conundrum of roaming environmental sensing by employing a terrestrial hermit crab (*Coenobita* spp.) as a native fauna partner to courier sensor and electronic payloads *via* a detachable harness. Using thermoforming to capture the initial harness profile followed by modification and 3D printing, the harness was a universal fit for a variety of shell sizes. The universal design of the harness allows it to be mounted on the hermit crab with minimum distress. It was able to withstand a tug force of up to 1 N. The robustness of the sensor and electronics enclosure on the harness was given an ingress protection rating of IP53 after tests. The hermit crab's suitability for the task was demonstrated with three types of sensor and electronic payload on its harness. It was able to courier a custom-designed LED electronic circuit, a commercially available solar-powered sensor with live wireless transmission of temperature and relative humidity, and a custom-designed salt water sensing module to successfully map the salt water boundary within an arena. While there are still challenges pertaining to the recovery of the harness and payload, the study has demonstrated a harness and customized sensing payload design strategy that allows us to partner with hermit crabs for opportunistic coastal environmental monitoring.

Data availability

The data from saltwater conductivity calibration, pendulum test and salt water sensor module characterization are provided in the ESI.† The video files for the five arena tests are available upon request.

Author contributions

BML: conceptualization, methodology, investigation, and writing – original draft. HKHL: formal analysis and validation. AS: conceptualization, validation, writing – review & editing, resources, and funding acquisition. BC: conceptualization, methodology, investigation, writing – original draft, writing – review & editing, and resources.

Conflicts of interest

The authors declare that they have no known competing financial interests or personal relationships that could have appeared to influence the work reported in this paper.

Acknowledgements

This work was supported by the National Research Foundation of Korea (grant number RS-2024-00333925).



References

- 1 Y. Li, Y. Hu, C. Yan, J. Xiong and Q. Qiu, *Appl. Soil Ecol.*, 2022, **175**, 104463.
- 2 C. Grenier, R. Román, C. Duarte, J. M. Navarro, A. B. Rodríguez-Navarro and L. Ramajo, *Environ. Pollut.*, 2020, **263**, 114555.
- 3 S. Akter, K. R. Ahmed, A. Marandi and C. Schüth, *Sci. Total Environ.*, 2020, **713**, 136668.
- 4 H. J. Lim, H. Jin, B. Chua and A. Son, *ACS Appl. Mater. Interfaces*, 2022, **14**, 4186–4196.
- 5 H. J. Lim, B. Chua and A. Son, *Biosens. Bioelectron.*, 2017, **94**, 10–18.
- 6 E.-H. Lee, H. J. Lim, A. Son and B. Chua, *Analyst*, 2015, **140**, 7776–7783.
- 7 K. A. Mitchell, B. Chua and A. Son, *Biosens. Bioelectron.*, 2014, **54**, 229–236.
- 8 M. S. Mannoor, S. Zhang, A. J. Link and M. C. McAlpine, *Proc. Natl. Acad. Sci. U. S. A.*, 2010, **107**, 19207–19212.
- 9 R. B. Clark and J. E. Dick, *ACS Sens.*, 2020, **5**, 3591–3598.
- 10 I. Tien, J.-M. Lozano and A. Chavan, *Commun. Earth Environ.*, 2023, **4**, 96.
- 11 K. Kawabata, F. Takemura, T. Suzuki, K. Sawai, E. Kuraya, S. Takahashi, H. Yamashiro, N. Isomura and J. Xue, *Int. J. Distributed Sens. Netw.*, 2014, **10**, 835642.
- 12 D. Ventura, M. Bruno, G. J. Lasinio, A. Belluscio and G. Ardizzone, *Estuar. Coast Shelf Sci.*, 2016, **171**, 85–98.
- 13 M. R. Palmer, Y. W. Shagude, M. J. Roberts, E. Popova, J. U. Wihsgott, S. Aswani, J. Coupland, J. A. Howe, B. J. Bett, K. E. Osuka, C. Abernethy, S. Alexiou, S. C. Painter, J. N. Kamau, N. Nyandwi and B. Sekadende, *Ocean Coast Manag.*, 2021, **212**, 105805.
- 14 S. Carpin and G. Pillonetto, Robot motion planning using adaptive random walks, *2003 IEEE International Conference on Robotics and Automation (Cat. No.03CH37422)*, Taipei, Taiwan, 2003, vol. 3, pp. 3809–3814, DOI: [10.1109/ROBOT.2003.1242181](https://doi.org/10.1109/ROBOT.2003.1242181).
- 15 B. Pang, Y. Song, C. Zhang, H. Wang and R. Yang, *J. Robot.*, 2019, **2019**, 6914212.
- 16 M. L. Casazza, A. A. Lorenz, C. T. Overton, E. L. Matchett, A. L. Mott, D. A. Mackell and F. McDuie, *J. Environ. Manage.*, 2023, **345**, 118636.
- 17 G. P. Mesquita, M. Mulero-Pázmány, S. A. Wich and J. D. Rodríguez-Teijeiro, *Curr. Zool.*, 2023, **69**, 208–214.
- 18 F. Roquet, C. Wunsch, G. Forget, P. Heimbach, C. Guinet, G. Reverdin, J.-B. Charrassin, F. Bailleul, D. P. Costa, L. A. Huckstadt, K. T. Goetz, K. M. Kovacs, C. Lydersen, M. Biuw, O. A. Nøst, H. Bornemann, J. Ploetz, M. N. Bester, T. McIntyre, M. C. Muelbert, M. A. Hindell, C. R. McMahon, G. Williams, R. Harcourt, I. C. Field, L. Chafik, K. W. Nicholls, L. Boehme and M. A. Fedak, *Geophys. Res. Lett.*, 2013, **40**, 6176–6180.
- 19 Z. Jagiello, Ł. Dylewski and M. Szulkin, *Sci. Total Environ.*, 2024, **913**, 168959.
- 20 Y. Kwak, S. M. Park, Z. Ku, A. Urbas and Y. L. Kim, *Nano Lett.*, 2021, **21**, 921–930.
- 21 D. Zhou, T. Lu, R. Sun and J. Zhang, *Crystals*, 2022, **12**, 234.
- 22 F. Marin and G. Luquet, *C. R. Palevol*, 2004, **3**, 469–492.
- 23 C. Bartlett, *Nexus Netw. J.*, 2019, **21**, 641–656.
- 24 K. A. C. Allsay and E. D. S. Dwi, *BIO Web Conf.*, 2023, **70**, 03003.
- 25 G.-W. Lee, T.-H. Kim, J.-H. Yun, N.-J. Kim, K.-H. Ahn and M.-S. Kang, *Front. Mater.*, 2023, **10**, DOI: [10.3389/fmats.2023.1183816](https://doi.org/10.3389/fmats.2023.1183816).
- 26 L. Albert, F. Olivier, A. Jolivet, L. Chauvaud and S. Chauvaud, *Mar. Environ. Res.*, 2023, **190**, 106106.
- 27 L. Albert, F. Deschamps, A. Jolivet, F. Olivier, L. Chauvaud and S. Chauvaud, *Mar. Environ. Res.*, 2020, **159**, 104958.
- 28 D. Lee and B. Chua, *Chem. Eng. J.*, 2023, **477**, 146949.
- 29 H. Xiang, Z. Li, H. Liu, T. Chen, H. Zhou and W. Huang, *npj Flexible Electron.*, 2022, **6**, 15.
- 30 S.-H. Lu, Y. Li and X. Wang, *J. Mater. Chem. B*, 2023, **11**, 7334–7343.
- 31 H. Qin, Z. Wang, Q. Yu, Q. Xu and X.-Y. Hu, *Sens. Actuators, B*, 2022, **371**, 132468.
- 32 S. Zhao, J. Li, D. Cao, G. Zhang, J. Li, K. Li, Y. Yang, W. Wang, Y. Jin, R. Sun and C.-P. Wong, *ACS Appl. Mater. Interfaces*, 2017, **9**, 12147–12164.
- 33 S. Yu, Y. Xu, Z. Cao, Z. Huang, H. Wang, Z. Yan, C. Wei, Z. Guo, Z. Chen, Y. Zheng, Q. Liao, X. Liao and Y. Zhang, *Adv. Funct. Mater.*, 2024, 2416984.
- 34 Z. Cao, Y. Xu, S. Yu, Z. Huang, Y. Hu, W. Lin, H. Wang, Y. Luo, Y. Zheng, Z. Chen, Q. Liao and X. Liao, *Adv. Funct. Mater.*, 2025, **35**, 2412649.
- 35 Z. Huang, S. Yu, Y. Xu, Z. Cao, J. Zhang, Z. Guo, T. Wu, Q. Liao, Y. Zheng, Z. Chen and X. Liao, *Adv. Mater.*, 2024, **36**, 2407329.
- 36 J. Sun, D. Ye, J. Zou, X. Chen, Y. Wang, J. Yuan, H. Liang, H. Qu, J. Binner and J. Bai, *J. Mater. Sci. Technol.*, 2023, **138**, 1–16.
- 37 Y. Yang, L. Zhang, J. Zhang, Y. Ren, H. Huo, X. Zhang, K. Huang, M. Rezakazemi and Z. Zhang, *Adv. Compos. Hybrid Mater.*, 2023, **6**, 140.
- 38 D. Lee and B. Chua, *ACS Appl. Mater. Interfaces*, 2021, **13**, 43984–43992.
- 39 D. Lee and B. Chua, *Sens. Actuators, A*, 2019, **290**, 80–89.
- 40 Y. Yang, B. Sun, X. Zhao, H. Yu, B. Wang, J. Li, Y. Tong, Q. Tang and Y. Liu, *J. Mater. Chem. C*, 2023, **11**, 8808–8817.
- 41 I. K. Ilic, V. Galli, L. Lamanna, P. Cataldi, L. Pasquale, V. F. Annese, A. Athanassiou and M. Caironi, *Adv. Mater.*, 2023, **35**, 2211400.

